Photochemical Studies of the Alkylammonium Molybdates. Part 7.* Octahedral Sites for Multi-electron Reduction of $[Mo_8O_{26}(MoO_4)_2]^{8-}$ †

Toshihiro Yamase
Research Laboratory of Resources Utilization, Tokyo Institute of Technology, 4259 Nagatsuta, Midori-ku, Yokohama, 227, Japan

Single-crystal e.s.r. spectra of u.v.-irradiated octakis(methylammonium) decamolybdate(VI) dihydrate, $[NH_3Me]_8[Mo_8O_{26}(MoO_4)_2]\cdot 2H_2O$, show the formation of two distinct localized $Mo^VO_5(OH)$ sites, resulting from a hydrogen-bonding proton transfer from $[NH_3Me]^+$ to a bridging oxygen atom in the anion. Analysis of the e.s.r. parameters g, $^{95,97}Mo$ hyperfine structure, and ^1H superhyperfine structure indicates the direct participation of the H 1*s* orbital in the semi-occupied molecular orbital with a spin population of 0.96—0.97 in Mo 4*d* orbitals. From the direction of the maximum principal value of the ^1H superhyperfine tensor, which lies close to the $Mo^V \cdots H^+(O)$ direction, two paramagnetic sites in the anion are determined and discussed in terms of the probability of the charge-transfer complex formation. One site has an arrangement of a MoO_4 group and two terminal oxygen atoms (*cis*-dioxo-group) about the central molybdenum atom and another is composed of one terminal and five bridging oxygen atoms. It is suggested that $[Mo_8O_{26}(MoO_4)_2]^{8-}$ suffers from the simultaneous multi-electron (up to four-electron) reduction photochemically.

In the course of our studies on the photochemistry of polyoxometalates which constitute an interesting family of potential photosensitizer and relay species in redox cycles (H_2 evolution from water and organic substances) for the chemical conversion of light energy,[1-7] photoreactive centres of the alkylammonium polymolybdates $[NH_3Pr^i]_6[Mo_8O_{26}(OH)_2]\cdot 2H_2O$ and $[NH_3Pr]_6[Mo_7O_{24}]\cdot 3H_2O$ have been investigated by single-crystal e.s.r. analyses.[8-12] The reduction of Mo^{VI} to Mo^V proceeds *via* photoexcitation of the oxygen-to-molybdenum charge-transfer band in a terminal Mo=O bond with an accompanying transfer of a hydrogen-bonding proton from alkylammonium nitrogen to a bridging oxygen atom, followed by an interaction of the non-bonding electrons of the amino-nitrogen with the terminal oxo-group leading to a charge-transfer complex (**1**) as shown in reaction (1).

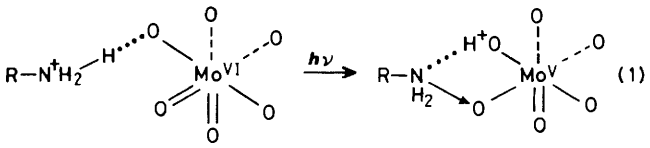

(1)

(1)

Single crystal e.s.r. spectra of the u.v.-irradiated alkylammonium polyoxomolybdates at room temperature show the formation of a localized Mo^V site. Based on the analysis of e.s.r. parameters, the paramagnetic site in the anion has been determined in conjunction with the *X*-ray structural data. The Mo^V site in the $[Mo_8O_{26}(OH)_2]^{6-}$ lattice has been observed at the octahedral site where the molybdenum atom originally coordinates a hydroxide group.[8] The Mo^V formation in the $[Mo_7O_{24}]^{6-}$ lattice occurs at an end of three octahedra on line with the central horizontal level of the $[Mo_7O_{24}]^{6-}$ polyhedral configuration.[10] Studies of the paramagnetic sites in the polyoxoanions have been extended to decamolybdate $[Mo_{10}O_{34}]^{8-}$. The atomic arrangement of this anion is shown in Figure 1.[13] The structural configuration of the $[Mo_{10}O_{34}]^{8-}$ lattice, which is equivalent to $[Mo_8O_{26}(MoO_4)_2]^{8-}$, having an

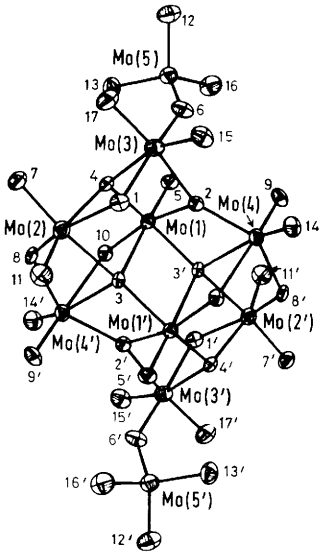

Figure 1. Structure of $[Mo_{10}O_{34}]^{8-}$ with the atom numbering scheme for the atoms

arrangement of eight edge-shared distorted MoO_6 octahedra linked by a pair of distorted MoO_4 tetrahedra, is the same as that of dihydrogen octamolybdate, $[Mo_8O_{26}(OH)_2]^{6-}$, which was found by us.[9] Although structurally very similar, $[Mo_8O_{26}(MoO_4)_2]^{8-}$ in this work is a linkage isomer of the decamolybdate reported by Fuchs *et al.*[14] These two decamolybdates can be distinguished by a different linkage of the MoO_4 groups. This paper describes an e.s.r. study on multi-electron (up to four-electron) reduction sites in the decamolybdate $[Mo_{10}O_{34}]^{8-}$ lattice. It is also interesting to know whether the tetrahedral MoO_4 site in $[Mo_8O_{26}(MoO_4)_2]^{8-}$ is a paramagnetic centre or not, since both anions of $[Mo_8O_{26}(OH)_2]^{6-}$ and $[Mo_7O_{24}]^{6-}$, in which the paramagnetic site has been studied, have an arrangement of condensed edge-shared octahedra only.

* Part 6 is ref. 10.
† *Non-S.I. unit employed:* G = 10^{-4} T.

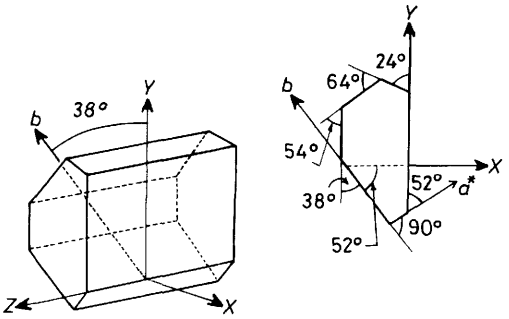

Figure 2. Idealized single crystal of $[NH_3Me]_8[Mo_{10}O_{34}]\cdot 2H_2O$

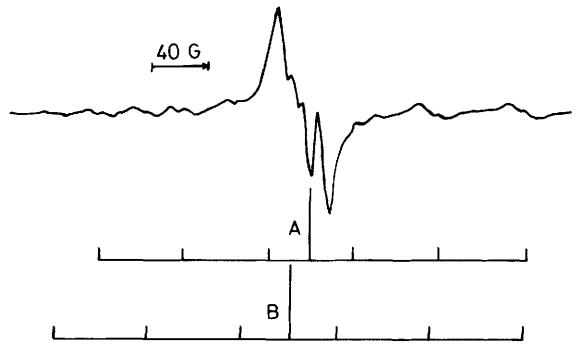

Figure 3. Example of e.s.r. spectrum obtained with a u.v.-irradiated crystal of $[NH_3Me]_8[Mo_{10}O_{34}]\cdot 2H_2O$ at room temperature. H_0 is in the ZX plane making 20° with the X axis; A and B correspond to the two paramagnetic sites

Experimental

Octakis(methylammonium) decamolybdate(VI) dihydrate $[NH_3Me]_8[Mo_{10}O_{34}]\cdot 2H_2O$ was obtained by the method previously described.[6] Single crystals were grown by slow evaporation from aqueous solutions at room temperature. Well developed colourless crystals of approximate dimensions 3 × 2 × 1 mm were obtained. The crystal is monoclinic with a = 12.596, b = 17.175, c = 10.653 Å, β = 91.40°, Z = 2, and space group $P2_1/n$ (data from ref. 13). The two molecules in the unit cell, being related by a centre of inversion, are magnetically equivalent. A crystal was irradiated at room temperature with u.v. light (λ ≥ 313 nm) from a 500-W super-high-pressure mercury lamp in conjunction with filters. After *ca.* 30 min of irradiation, the crystal, which is reddish brown, was mounted on a quartz rod using silicon grease. E.s.r. experiments were performed on a Varian E-12 spectrometer at X-band frequency (100-kHz field modulation). Diphenylpicrylhydrazyl was used as a field marker. Spectra were recorded at intervals of 10°, as the magnet was rotated about each of the orthogonal axes X, Y, and Z to which our results were referred. After completion of e.s.r. measurements the orientation of the body-fixed orthogonal axes with respect to the crystallographic axes was determined by both oscillation and Weissenberg photographs. An idealized representation of the u.v.-irradiated single crystal of $[NH_3Me]_8[Mo_{10}O_{34}]\cdot 2H_2O$ is given in Figure 2, together with the crystallographic axes. The Z axis is coincident with the crystallographic c^* axis. The axes Y and Z lie in the flat face of the crystal perpendicular to the X axis making an angle of 38° with the a^* axis.

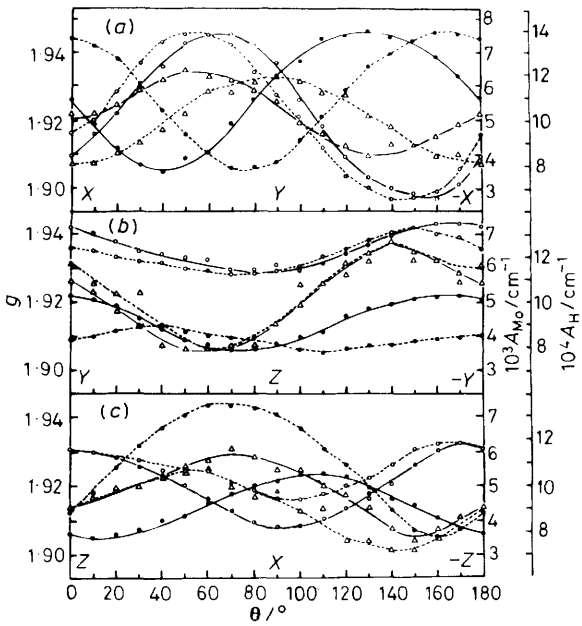

Figure 4. Angular dependences of the signals A (——) and B (– – – –) in the XY (*a*), YZ (*b*), and ZX (*c*) planes: g (○), A_{Mo} (●), and A_H (△)

Results

The spectrum obtained with a u.v.-irradiated single crystal of $[NH_3Me]_8[Mo_{10}O_{34}]\cdot 2H_2O$ reveals the presence of two paramagnetic sites $Mo^V(OH)$, A and B, as shown in Figure 3. The spectrum of each Mo^V centre consists of two sets of lines: a doublet and a sextet of doublets. The first set of lines is attributed to the interaction (*ca.* 10 G) of the unpaired electron with a ^1H nucleus ($I = \frac{1}{2}$). The nature of this more intense set of lines corresponds to the ^{96}Mo atom ($I = 0$). The second set of lines, of less intensity, characterizes the hyperfine spectrum of ^{95}Mo and ^{97}Mo further split by the same superhyperfine interaction of the first set of lines. The relative intensity of the two sets of lines agrees well with the molybdenum isotopic composition. The two molybdenum isotopes, $^{95,97}Mo$, in total natural abundance (25.15%) have the same nuclear spin ($I = \frac{5}{2}$) and nearly the same magnetic moment, so that it is not possible to resolve the separate hyperfine lines. The spectrum has been interpreted using the spin-Hamiltonian [equation (2)] with $S = \frac{1}{2}$, $I_{Mo} = \frac{5}{2}$, and $I_H = \frac{1}{2}$.

$$\mathcal{H} = \beta g H S + A_{Mo} I_{Mo} S + A_H I_H S \qquad (2)$$

Figure 4 shows the angular variation of the e.s.r. spectrum of the sites A and B for the rotation of the magnetic field in the planes XY, YZ, and ZX. The e.s.r. tensors g, A_{Mo}, and A_H have been obtained using successively a least-squares fitting sub-routine and performing a direct diagonalization of the Hamiltonian. We have previously described this procedure elsewhere.[8] The results are given in Table 1. Two sets of tensors, g, A_{Mo}, and A_H, can be referred to two magnetically inequivalent paramagnetic sites A and B in the unit cell, where two molecules are magnetically equivalent as related by a centre of inversion.[13] For two sets of tensors of sites A and B, similar eigenvalues are obtained. It is interesting to compare the present results with those previously obtained for $[NH_3Pr^i]_6[Mo_8O_{26}(OH)_2]\cdot 2H_2O$[8] and $[NH_3Pr]_6[Mo_7O_{24}]\cdot 3H_2O$.[10] Table 2 summarizes e.s.r. parameters for each paramagnetic centre in two lattices, $[Mo_8O_{26}(OH)_2]^{6-}$ and $[Mo_7O_{24}]^{6-}$. It can be seen readily that the parameters found in the present work are at first sight quite compatible with those for the octahedral Mo^V site in $[Mo_8O_{26}(OH)_2]^{6-}$ or $[Mo_7O_{24}]^{6-}$. This indicates that the choice of sign for the tensor components of the sites A and B is the same as that for the Mo^V site in $[Mo_7O_{24}]^{6-}$, which gives

Table 1. Electron spin resonance tensors for two Mo^{V} centres A and B

Principal values		Direction cosines with respect to X	Y	Z	Principal values		Direction cosines with respect to X	Y	Z
Site A					Site B				
g^a g_1	1.899	−0.9047	0.4223	0.0567	g_1	1.899	−0.8156	0.5728	0.0827
g_2	1.930	±0.1003	±0.0818	±0.9916	g_2	1.930	±0.1709	±0.1020	±0.9800
g_3	1.949	0.4141	0.9028	0.1164	g_3	1.949	0.5529	0.8133	−0.1811
g_o	1.926				g_o	1.926			
$A_{Mo}{}^b$ $A_{Mo(1)}$	23.7	0.6316	0.5757	0.5193	$A_{Mo(1)}$	28.0	0.3533	0.6306	−0.6911
$A_{Mo(2)}$	40.2	∓0.3791	∓0.3549	±0.8546	$A_{Mo(2)}$	41.8	−0.0312	0.7462	0.6650
$A_{Mo(3)}$	73.5	−0.6763	0.7366	0.0059	$A_{Mo(3)}$	76.8	−0.9350	0.2134	−0.2833
A_{MoO}	45.8				A_{MoO}	48.9			
$A_H{}^c$ $A_{H(1)}$	6.57	−0.4350	0.5485	0.7141	$A_{H(1)}$	6.87	−0.6521	0.2462	0.7170
$A_{H(2)}$	10.7	∓0.7657	±0.1919	∓0.6139	$A_{H(2)}$	9.69	∓0.7424	∓0.3993	∓0.5380
$A_{H(3)}$	12.4	0.4737	0.8139	−0.3365	$A_{H(3)}$	12.3	−0.1539	0.8831	−0.4432
A_{HO}	9.86				A_{HO}	9.63			

[a] $g_o = (g_1 + g_2 + g_3)/3$. [b] Units in 10^{-4} cm^{-1}; $A_{MoO} = [A_{Mo(1)} + A_{Mo(2)} + A_{Mo(3)}]/3$. [c] Units in 10^{-4} cm^{-1}; $A_{HO} = [A_{H(1)} + A_{H(2)} + A_{H(3)}]/3$.

Table 2. Electron spin resonance parameters of Mo^{V} centres in other kinds of polyoxomolybdates

Principal values		$[NH_3Pr^i]_6$-$[Mo_8O_{26}(OH)_2]\cdot 2H_2O$ [a]	$[NH_3Pr]_6$-$[Mo_7O_{24}]\cdot 3H_2O$ [b]
g	g_1	1.897	1.895
	g_2	1.941	1.925
	g_3	1.955	1.937
	g_O	1.931	1.919
A_{Mo}	$A_{Mo(1)}$	[c]	23.4
	$A_{Mo(2)}$	[c]	42.0
	$A_{Mo(3)}$	[c]	69.9
	A_{MoO}	[c]	45.1
A_H	$A_{H(1)}$	8.69 [d]	8.15
	$A_{H(2)}$	9.28	9.14
	$A_{H(3)}$	10.1	12.5
	A_{HO}	9.37	9.93

[a] From ref. 8. [b] From ref. 10. [c] The signals due to $^{95,97}Mo$ hyperfine structure were too weak to analyze at all orientations. [d] In ref. 8 a choice of signs for ^1H tensors was not made.

the total spin density closest to unity. It is this one which we report in Table 1.

The relative magnitude of the components of the g tensor shows $g_\perp > g_\parallel$, if $g_\perp = (g_2 + g_3)/2$ and $g_\parallel = g_1$ are assumed. This can be explained by a small value (152 cm^{-1}) of the spin–orbit coupling constant for oxygen atoms bonded to molybdenum.[15] The plot of the angular dependence of the g values for the site A, in the crystal XY plane, reaches a maximum (1.945) at *ca.* 70° from the X axis and for the site B at *ca.* 50° from the X axis. The value almost approaches the highest of the principal g values, g_3 (1.949); hence these directions in the XY plane approach the g_3 vector directions for the two sites. In the XY plane, furthermore, at *ca.* 70 and 50° from the Y axis, the minimum values (*ca.* 1.897) are obtained for the sites A and B, respectively. The values approach $g_1 = 1.899$; hence these directions could be considered nearly coincident with the directions of g_1 for the two sites. Similarly, the plots of the angular dependence of A_{Mo} values in the crystal XY plane give their maximum values (76.4 × 10^{-4} and 75.8 × 10^{-4} cm^{-1}) at *ca.* 40 and 70° from the Y axis for the sites A and B respectively. These directions approach the $A_{Mo(3)}$ vector directions for the two sites. The plot of the angular dependence of the A_{Mo} values in the YZ plane for the site B shows their maximum, A_{Mo} = 42.8 × 10^{-4} cm^{-1} at *ca.* 40° from the Y axis. The value is close to $A_{Mo(2)}$ = 41.8 × 10^{-4} cm^{-1}; hence this direction in the YZ plane approaches the $A_{Mo(2)}$ vector direction. In addition the plots of the angular dependence of A_H values in the XY plane give their maximum values (12.2 × 10^{-4} and 11.9 × 10^{-4} cm^{-1}) at *ca.* 40 and 10° from the Y axis for the sites A and B, respectively. Furthermore, the angular variation of A_H values in the YZ plane gives their maximum value (12.7 × 10^{-4} cm^{-1}) at *ca.* 140° from the Y axis for the two sites and the value is close to $A_{H(3)}$. These directions in the XY and YZ planes approach the $A_{H(3)}$ vector directions. Table 1 shows the direction cosines of the tensor values which give the best fit based on the above considerations. The non-coincidence of principal axes of the g and A tensors (Table 1) originates in the extensive d-orbital mixing allowed by the low-symmetry ligand field in the site, indicating the displacement of the directions of the principal g values from the Mo–O axis.

Discussion

The principal values (10^{-4} cm^{-1}) of the $^{95,97}Mo$ hyperfine tensors are 23.7, 40.2, and 73.5 for the site A (28.0, 41.8, and 76.8 for the site B). To a good approximation, therefore, the hyperfine tensors are axial with $A_{Mo\parallel}$ = 73.5 × 10^{-4} cm^{-1} (76.8 × 10^{-4} cm^{-1} for site B) and $A_{Mo\perp}$ = 31.9 × 10^{-4} cm^{-1} (34.9 × 10^{-4} cm^{-1} for site B). Defining an anisotropic hyperfine parameter for d orbitals as $7(A_{Mo\parallel} - A_{Mo\perp})/6$ and dividing its value, 48.3 × 10^{-4} cm^{-1} (49.0 × 10^{-4} cm^{-1}), by the anisotropic hyperfine parameter $P = g\beta\gamma_{Mo}\langle r^{-3}\rangle_{4d}$ for $^{95,97}Mo$ (150.7 MHz [16] ≡ 50.3 × 10^{-4} cm^{-1}) gives an estimate of 0.96 (0.97 for site B) for the spin population in Mo 4d orbitals, when $A_{Mo\parallel}$ and $A_{Mo\perp}$ have the same sign.[10] If $A_{Mo\parallel}$ and $A_{Mo\perp}$ are assumed to have opposite signs an estimated Mo(4d) contribution of 2.55 is obtained. This constitutes an unacceptably large total spin density and strongly implies that $A_{Mo\parallel}$ and $A_{Mo\perp}$ have the same sign. The $^{95,97}Mo$ isotropic hyperfine interaction is equal to 45.8 × 10^{-4} cm^{-1} for site A (48.9 × 10^{-4} cm^{-1} for site B). The isotropic hyperfine interaction for unit spin density in a Mo 5s orbital, which is obtained by computing the isotropic hyperfine interaction $A = (8\pi g\beta\gamma/3)\psi^2(0)$, is 66.2 × 10^{-3} cm^{-1}, where $\psi^2(0)$ is the atomic parameter;[10,16] hence a Mo(5s) contribution of 0.07 for each of two sites is indicated.

Since the physically most reasonable choice of sign for ^1H superhyperfine tensor components is positive, as discussed in a previous paper,[10] a H(1s) contribution of 0.02 may be derived from dividing A_{HO} = 9.86 × 10^{-4} cm^{-1} (9.63 × 10^{-4} cm^{-1} for site B) by the isotropic hyperfine interaction, 474 × 10^{-4} cm^{-1}

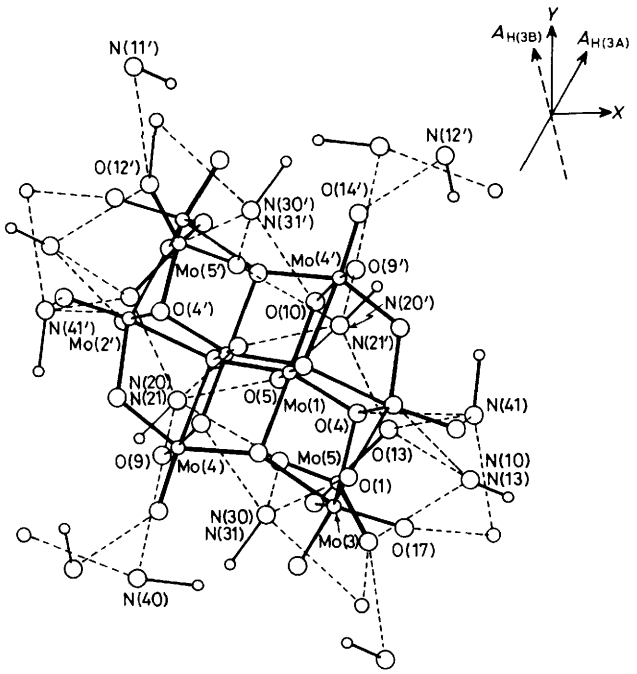

Figure 5. Molecular structure of $[NH_3Me]_8[Mo_{10}O_{34}]$, viewed in projection along the Z axis. $A_{H(3A)}$ and $A_{H(3B)}$ denote the principal $A_{H(3)}$ directions of the sites A and B in the XY plane, respectively

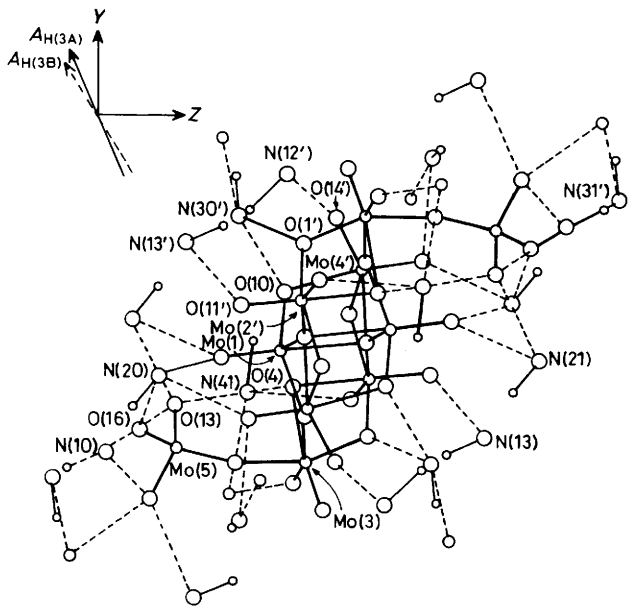

Figure 6. Molecular structure of $[NH_3Me]_8[Mo_{10}O_{34}]$, viewed in projection along the X axis. $A_{H(3A)}$ and $A_{H(3B)}$ denote the principal $A_{H(3)}$ directions of the sites A and B in the YZ plane, respectively

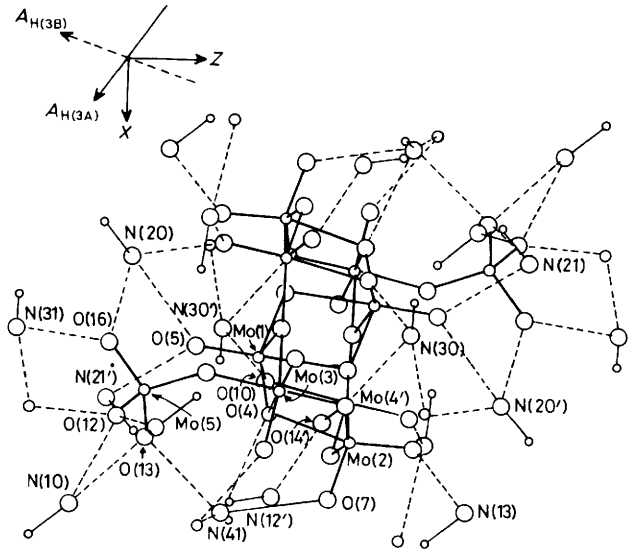

Figure 7. Molecular structure of $[NH_3Me]_8[Mo_{10}O_{34}]$, viewed in projection along the Y axis. $A_{H(3A)}$ and $A_{H(3B)}$ denote the principal $A_{H(3)}$ directions of the sites A and B in the ZX plane, respectively

(ref. 17) for unit spin density in the 1s orbital of a H atom.[10] The total spin density for site A is therefore 0.96 + 0.07 + 0.02 = 1.05 (1.06 for site B), a reasonably satisfactory result.

The positive sign of the ^1H superhyperfine tensors indicates that the H 1s orbital participates directly in the semi-occupied molecular orbital and that the highest of the principal values, $A_{H(3)} = 12.4 \times 10^{-4}$ cm^{-1} for site A (12.3×10^{-4} cm^{-1} for site B), is approximately parallel to the $Mo^V \cdots H^+(O)$ direction.[10,18] The proton at the photoreduced MoO_6 site in u.v.-irradiated specimens of $[NH_3Pr^i]_6[Mo_8O_{26}(OH)_2]\cdot 2H_2O$ and $[NH_3Pr]_6[Mo_7O_{24}]\cdot 3H_2O$ was derived from the transfer of the alkylammonium hydrogen-bonding proton to the bridging oxygen atom, which resulted from the photoexcitation of the ligand to metal charge-transfer (l.m.c.t.) band of the terminal Mo=O bond [equation (1)].[8,10] The hydrogen-bonding proton at the Mo^V site of the photoreduced $[Mo_{10}O_{34}]^{8-}$ would be situated around the N ··· O line in the range between one-quarter and three-quarters of the N ··· O distance (2.77—3.20 Å)[13] from the oxygen atom, in conjunction with the fact that methylammonium N^+–H and hydroxide O–H distances are 0.68—0.83 Å[13] and 0.82 Å* respectively. Since there was no significant change in both the i.r. spectra and powder X-ray diffraction patterns between non-irradiated and irradiated samples, it is assumed that the structure of the parent oxidized form is retained upon irradiation, as proposed in the solid-state photochemistry of $[NH_3Pr]_6[Mo_7O_{24}]\cdot 3H_2O$.[10] Thus, the present e.s.r. results are in agreement with the site symmetry determined for $[Mo_{10}O_{34}]^{8-}$. This enables us to determine the paramagnetic sites in the anion.

The molecule viewed in projection along X, Y, and Z axes is represented together with the principal $A_{H(3)}$ directions in Figures 5—7, where dotted lines indicate the N ··· O distance of 2.77—3.20 Å, with the involvement of a hydrogen-bonding proton. The Mo sites, in which the $Mo \cdots H^+(O)$ direction appears to be well in accord with the direction of the $A_{H(3)}$ vector for each of Figures 5—7, are given in Table 3. Table 3 allows us assign the paramagnetic site A to either $Mo(3) \cdots H^+[O(4) \cdots N(41)]$ or $Mo(4') \cdots H^+[O(14') \cdots N(12')]$ and the site B to $Mo(1) \cdots H^+[O(10) \cdots N(30')]$. Any other Mo sites are extremely improbable. For example, the $Mo(4) \cdots H^+[O(9) \cdots N(40)]$ direction is in good agreement with the $A_{H(3)}$ vector direction for the site A in the XY plane, but lies almost perpendicular to the $A_{H(3)}$ vector the YZ plane. This indicates that the possibility of the $Mo(4) \cdots H^+[O(9) \cdots N(40)]$ as site A can be excluded. It is to be noted that the tetrahedral Mo(5) site is unlikely to be reduced. Figure 8 shows the arrangement of the six O atoms and N atom about each of the MoO_6 sites: Mo(1), Mo(3), and Mo(4'). The Mo(3) or Mo(4') atom is surrounded by a distorted octahedral set of six O

* A hydroxide O–H distance of 0.82 Å is observed for $[Mo_8O_{26}(OH)_2]^{6-}$.[9]

Table 3. $Mo^{V} \cdots H^{+}$ directions close to the $A_{H(3)}$ vector direction with the molecule projected on three planes[a]

Plane	Plausible directions[b] Site A	Site B
XY	Mo(1) ··· H⁺[O(5) ··· N(20,21)]	Mo(1) ··· H⁺[O(10) ··· N(30′,31′)]
	Mo(2′) ··· H⁺[O(4′) ··· N(41′)]	Mo(2′) ··· H⁺[O(4′) ··· N(41′)]
	Mo(3) ··· H⁺[O(4) ··· N(41)]	Mo(3) ··· H⁺[O(1) ··· N(30,31)]
	Mo(4) ··· H⁺[O(9) ··· N(40)]	Mo(4) ··· H⁺[O(9) ··· N(20)]
	Mo(4′) ··· H⁺[O(14′) ··· N(12′)]	Mo(5′) ··· H⁺[O(12′) ··· N(11′)]
	Mo(5) ··· H⁺[O(13) ··· N(20′,21′)]	
YZ	Mo(1) ··· H⁺[O(10) ··· N(30′)]	Mo(1) ··· H⁺[O(10) ··· N(30′)]
	Mo(2′) ··· H⁺[O(1′) ··· N(30′)]	Mo(2′) ··· H⁺[O(1′) ··· N(30′)]
	Mo(2′) ··· H⁺[O(11′) ··· N(13′)]	Mo(2′) ··· H⁺[O(11′) ··· N(13′)]
	Mo(3) ··· H⁺[O(4) ··· N(41)]	Mo(3) ··· H⁺[O(4) ··· N(41)]
	Mo(4′) ··· H⁺[O(14′) ··· N(12′)]	Mo(4′) ··· H⁺[O(14′) ··· N(13′)]
	Mo(5) ··· H⁺[O(13) ··· N(10)]	Mo(5) ··· H⁺[O(13) ··· N(10)]
	Mo(5) ··· H⁺[O(16) ··· N(20)]	Mo(5) ··· H⁺[O(16) ··· N(20)]
ZX	Mo(1) ··· H⁺[O(10) ··· N(30′)]	Mo(1) ··· H⁺[O(5) ··· N(20)]
	Mo(2) ··· H⁺[O(7) ··· N(41)]	Mo(1) ··· H⁺[O(10) ··· N(30′)]
	Mo(3) ··· H⁺[O(4) ··· N(41)]	Mo(2) ··· H⁺[O(4) ··· N(41)]
	Mo(4′) ··· H⁺[O(14′) ··· N(12′)]	Mo(4) ··· H⁺[O(9) ··· N(40)]
	Mo(5) ··· H⁺[O(12) ··· N(10)]	Mo(4′) ··· H⁺[O(10) ··· N(30′)]
	Mo(5) ··· H⁺[O(13) ··· N(12′)]	Mo(5) ··· H⁺[O(16) ··· N(31)]

[a] Mo ··· H⁺(O ··· N) denotes the $Mo^{V} \cdots H^{+}$ direction at the Mo^{V} site assumed when H^{+} transfers from the methylammonium N atom to the O atom at the photoreducible Mo site. [b] N(11)—(13), N(21)—(22), N(31), and N(41) denote N(1), N(2), N(3), and N(4) atoms in the adjacent unit cell, which are crystallographically equivalent to N(10), N(20), N(30), and N(40), respectively. Primed atoms are related to corresponding unprimed ones by an inversion centre in the anion (see Figure 1).

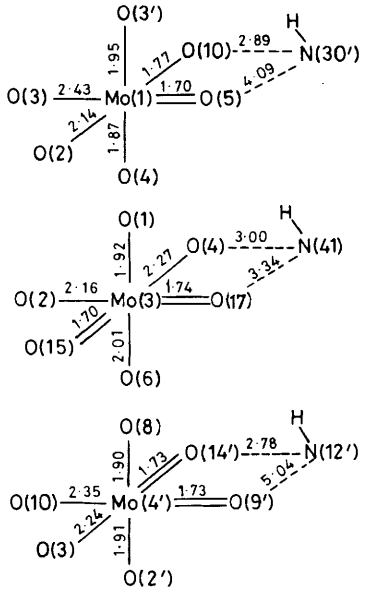

Figure 8. Interatomic distances (Å) including the Mo(1), Mo(3), and Mo(4′) sites

atoms, two of which are of terminal doubly bonded *cis*-dioxo-groups and four are bridging. This arrangement resembles the photoreducible MoO_6 sites in two anions, $[Mo_7O_{24}]^{6-}$ and $[Mo_8O_{26}(OH)_2]^{6-}$. On the other hand, Mo(1) is surrounded by one terminal doubly bonded oxygen [O(5)] and five bridging oxygen atoms. If the Mo(4′) centre is photoreducible, u.v.-induced formation of the charge-transfer complex (**1**) [equation (1)] may occur *via* proton transfer from the methylammonium N(12′) atom to the terminal O(14′) atom, followed by an interaction of the amino-N(12′) atom with the terminal O(9′) atom. However, the proton transfer from N(12′) to O(14′) is unlikely, because of the strong electrostatic repulsion between the proton and the photogenerated hole at O(14′); the latter results from the photoexcitation of the l.m.c.t. band of the terminal Mo=O bond, as well as at O(9′). Furthermore, it must be noted that the N(12′) ··· O(9′) separation of 5.04 Å[13] is very long, compared with the N(30′) ··· O(5) separation of 4.09 Å at the Mo(1) site or the N(41) ··· O(17) separation of 3.34 Å at the Mo(3) site. The long distance N(12′) ··· O(9′) leads to a lowering in the probability of the charge-transfer complex formation, resulting in a relative insensitivity to the photoreduction of the Mo(4′) site, as discussed previously.[10] E.s.r. signals (Figure 3) showed both ^{95,97}Mo-hyperfine and ^{1}H-superhyperfine structures without any exchange broadening, which were characteristic of the unpaired electron localized on one Mo site only.* Therefore the signals indicate the small extent of antiferromagnetic coupling of the two electrons at the adjacent edge-shared octahedral sites of $Mo^{V}(1)$ and $Mo^{V}(3)$ (Figure 1). This may be attributed to the significant departure of both Mo(1)–O(2)– Mo(3) (103.3°) and Mo(1)–O(4)–Mo(3) (108.7°) angles[13] from linearity. The conclusion that both Mo(1) and Mo(3) sites are photoreducible gives also paramagnetic sites at both Mo(1′) and Mo(3′), since the arrangement of polyhedra can be related by the inversion centre in the anion (Figure 1). This implies the occurrence of four separate and independent one-electron photoreductions at Mo(1), Mo(1′), Mo(3), and Mo(3′) in the $[Mo_{10}O_{34}]^{8-}$ anion. Non-linear arrangement of Mo(1)–O(3)– Mo(1′) (104.3°)[13] appears to be a factor for the localization of the unpaired electron at each Mo^{V} site of Mo(1) and Mo(1′), giving the observation of the two distinct sites for four-electron reduction of the anion.

In the light of the e.s.r. signals from the $Mo^{V}(1)$ and $Mo^{V}(3)$

* The 'hopping frequency' at room temperature must be much lower than *ca.* 2.0×10^{8} Hz (separation between $g_{\parallel}$ and $g_{\perp}$ expressed in frequency units).

sites in $[Mo_{10}O_{34}]^{8-}$, an alternative possibility is that the e.s.r. signals belong to the one-electron reduction at either the Mo(1) or Mo(3) site in the anion. If this is so, then two kinds of species of $Mo^{V}(1)$ and $Mo^{V}(3)$ must be randomly distributed over the whole lattice, since there was no significant difference in the signal intensities between the two sites. It should be remembered also that the rate of the u.v.-induced colouration due to Mo^{V} formation for the $[Mo_{10}O_{34}]^{8-}$ lattice was a few times higher than that of $[Mo_8O_{26}(OH)_2]^{6-}$ or $[Mo_7O_{24}]^{6-}$.[6,*] In conjunction with the similarity of absorption spectra ($\lambda_{max.}$ = 480—510 nm) among these u.v.-irradiated polyoxomolybdate solids,[6] therefore, high efficiency of the rate of the photocolouration of $[NH_3Me]_8[Mo_{10}O_{32}]\cdot 2H_2O$ solid strongly supports four separate and independent one-electron reductions of $[Mo_{10}O_{34}]^{8-}$. The non-observation of the tetrahedral $Mo^{V}(5)$ site can be explained by the electrostatic repulsion between the proton and the hole photogenerated at terminal O(12), O(13), and O(16) atoms (Figures 5—7), which gives little possibility of the proton transfer at the Mo(5) site resulting in the thermal deactivation to the original Mo=O state without any formation of the charge-transfer complex (**1**).

The geometry of the Mo(3) site in $[Mo_8O_{26}(MoO_4)_2]^{8-}$ resembles that of the photoreducible site in $[Mo_8O_{26}(OH)_2]^{6-}$, which was assigned to the site co-ordinating a hydroxide group.[8] On the pathway to the u.v.-induced formation of the charge-transfer complex (**1**) in equation (1), however, the Mo(3) site adopts a different mode (Figure 8); the proton-transfered bridging oxygen atom O(4) in $[Mo_{10}O_{34}]^{8-}$ lies *cis* to the Mo(3)–O(6)(MoO_6) bond [O(4)–Mo(3)–O(6) angle of 85.1°[13]], while the proton-transferred oxygen atom in $[Mo_8O_{26}(OH)_2]^{6-}$ lies *trans* to the Mo–OH bond (O–Mo–OH angle of 156.8°[9]).

Two distinct paramagnetic centres have also been observed for the u.v.-irradiated $[NH_3Pr^{i}]_6[Mo_7O_{24}]\cdot 3H_2O$ single crystal.[4] Unfortunately, the final R value of 0.060 for these structural data, making interatomic distances and angles of the hydrogen bonds uncertain, resulted in difficulty in the assignment of the photoreducible Mo site. On the other hand, the Mo^{V} formation in the $[NH_3Pr]_6[Mo_7O_{24}]\cdot 3H_2O$ crystal occurred at an end of three octahedra in a line in the central horizontal level of the $[Mo_7O_{24}]^{6-}$ configuration.[10] Therefore, it is suggested that the two paramagnetic Mo^{V} sites in $[NH_3Pr^{i}]_6[Mo_7O_{24}]\cdot 3H_2O$ (space group $P2/n$, $Z = 4$)[11] belong to two ends (two-electron reduction) of three octahedra in the central level of $[Mo_7O_{24}]^{6-}$ or one at an alternative end (one-electron reduction), which must be randomly distributed over the lattice.

* 'MAM,' 'IPAM,' 'PAM,' and '6IAP8M2' in ref. 6 refer to the compounds $[NH_3Me]_8[Mo_{10}O_{34}]\cdot 2H_2O$, $[NH_3Pr^{i}]_6[Mo_7O_{24}]\cdot 3H_2O$, $[NH_3Pr]_6[Mo_7O_{24}]\cdot 3H_2O$, and $[NH_3Pr^{i}]_6[Mo_8O_{26}(OH)_2]\cdot 2H_2O$ respectively.

Acknowledgements

I wish to thank Mr. Y. Sasaki for his help in taking projections of the molecular structure on the planes.

References

1 T. Yamase, N. Takabayashi, and M. Kaji, *J. Chem. Soc., Dalton Trans.*, 1984, 793.
2 T. Yamase and T. Kurozumi, *Inorg. Chim. Acta*, 1984, **83**, L25; T. Yamase, *ibid.*, 1981, **54**, L165; 1982, **64**, L155; 1983, **76**, L25.
3 T. Yamase and T. Kurozumi, *J. Chem. Soc., Dalton Trans.*, 1983, 2205.
4 T. Yamase, R. Sasaki, and T. Ikawa, *J. Chem. Soc., Dalton Trans.*, 1981, 628.
5 T. Yamase, *Inorg. Chim. Acta*, 1981, **54**, L207; T. Yamase and T. Ikawa, *ibid.*, 1979, **37**, L529; 1980, **45**, L55.
6 T. Yamase and T. Ikawa, *Bull. Chem. Soc. Jpn.*, 1977, **50**, 746.
7 H. Toraya, F. Marumo, and T. Yamase, *Acta Crystallogr., Sect. B*, 1984, **40**, 145; P. K. Bharadwaj, Y. Ohashi, Y. Sasada, Y. Sasaki, and T. Yamase, *Acta Crystallogr., Sect. C*, 1984, **40**, 48; T. Yamase, T. Ikawa, Y. Ohashi, and Y. Sasada, *J. Chem. Soc., Chem. Commun.*, 1979, 697; T. Yamase, H. Hayashi, and T. Ikawa, *Chem. Lett.*, 1974, 1055; T. Yamase, T. Ikawa, H. Kokado, and E. Inoue, *ibid.*, 1973, 615.
8 T. Yamase, *J. Chem. Soc., Dalton Trans.*, 1978, 283.
9 M. Isobe, F. Marumo, T. Yamase, and T. Ikawa, *Acta Crystallogr., Sect. B*, 1978, **34**, 2728.
10 T. Yamase, *J. Chem. Soc., Dalton Trans.*, 1982, 1987.
11 Y. Ohashi, K. Yanagi, Y. Sasada, and T. Yamase, *Bull. Chem. Soc. Jpn.*, 1982, **55**, 1254.
12 T. Yamase, 'Proceedings of Climax Fourth International Conference on Chemistry and Uses of Molybdenum,' eds. H. F. Barry and P. C. H. Mitchell, Climax Molybdenum Co., Ann Arbor, Michigan, 1982, pp. 208–211.
13 Y. Sasaki, T. Yamase, P. K. Bharadwaj, Y. Ohashi, and Y. Sasada, *Acta Crystallogr., Sect. C*, in the press.
14 J. Fuchs, H. Hartl, W-D Hunnius, and S. Mahjour, *Angew. Chem.*, 1975, **87**, 634.
15 M. Che, M. Fournier, and J. P. Launay, *J. Chem. Phys.*, 1979, **71**, 1954; D. S. McClure, *ibid.*, 1949, **17**, 905.
16 J. R. Morton and K. F. Preston, *J. Magn. Reson.*, 1978, **30**, 577.
17 J. R. Morton, *Chem. Rev.*, 1964, **64**, 453; P. W. Atkins and M. C. R. Symons, 'The Structure of Inorganic Radicals,' Elsevier, Amsterdam, 1967, p. 24.
18 W. Derbyshire, *Mol. Phys.*, 1962, **5**, 225; D. Pooley and D. H. Whiffen, *Trans. Faraday Soc.*, 1961, **57**, 1445.

Received 18*th February* 1985; *Paper* 5/274